Polyhedron 38 (2012) 285–290

Contents lists available at SciVerse ScienceDirect

Polyhedron

journal homepage: www.elsevier.com/locate/poly

Complexation of 2-acetylpyridine- and 2-benzoylpyridine-derived hydrazones to copper(II) as an effective strategy for antimicrobial activity improvement

Angel A. Recio Despaigne [a], Fernanda B. Da Costa [a], Oscar E. Piro [b], Eduardo E. Castellano [c], Sonia R.W. Louro [d], Heloisa Beraldo [a,*]

[a] Departamento de Química, Universidade Federal de Minas Gerais, 31270-901 Belo Horizonte, MG, Brazil
[b] Departamento de Física, Facultad de Ciencias Exactas, Universidad Nacional de La Plata and Instituto IFLP (CONICET, CCT-La Plata), C.C. 67, 1900 La Plata, Argentina
[c] Instituto de Física de São Carlos, Universidade de São Paulo, C.P. 369, 13560-970 São Carlos, SP, Brazil
[d] Departamento de Física, Pontifícia Universidade Católica do Rio de Janeiro, 22453-900 Rio de Janeiro, Brazil

ARTICLE INFO

Article history:
Received 31 January 2012
Accepted 9 March 2012
Available online 17 March 2012

Keywords:
Hydrazones
Copper(II) complexes
Antimicrobial activity

ABSTRACT

Complexes [Cu(2AcPh)Cl]·2H_2O (**1**), [Cu(2Ac*p*ClPh)Cl]·2H_2O (**2**), [Cu(2Ac*p*NO_2Ph)Cl] (**3**), [Cu(2BzPh)Cl] (**4**). [Cu(2Bz*p*ClPh)Cl] (**5**) and [Cu(2Bz*p*NO_2Ph)Cl] (**6**) were obtained with 2-acetylpyridine-phenylhydrazone (H2AcPh), 2-acetylpyridine-*para*-chloro-phenylhydrazone (H2Ac*p*ClPh), 2-acetylpyridine-*para*-nitro-phenylhydrazone (H2Ac*p*NO_2Ph), 2-benzoylpyridine-phenylhydrazone (H2BzPh), 2-benzoylpyridine-*para*-chloro-phenylhydrazone (H2Bz*p*ClPh) and 2-benzoylpyridine-*para*-nitro-phenylhydrazone (H2Bz*p*NO_2Ph). The hydrazones showed poor antibacterial effect against *Staphylococcus aureus*, *Enterococcus faecalis* and *Pseudomonas aeruginosa* but demonstrated significant antifungal activity against *Candida albicans*. Upon coordination to copper(II) the antibacterial and antifungal activities appreciably increased. H2Ac*p*ClPh, H2Bz*p*ClPh and their copper(II) complexes (**2**) and (**5**), respectively, were as active as fluconazole against *C. albicans*.

1. Introduction

Hydrazones have attracted considerable attention due to their interesting chemical and structural properties. Their optical, thermal and photoelectrical properties have been reported in the literature [1]. They are employed in the polymer industry as plasticising agents, antioxidants and polymerisation initiators [2]. Hydrazone derivatives are reported to possess antimicrobial [3–5], antitubercular [6–8], anticonvulsant [9,10], anti-inflammatory [11,12], antiviral [13,14], and anti-proliferative [15,16] activities. In addition, some aroylhydrazones have shown cytotoxic activity and their binding to cellular Fe results in oxidative damage to vital bio-molecules [17]. Metal complexes of hydrazones also exhibit a wide range of pharmacological applications as antimicrobial [18–20], cytotoxic [21,22], and as DNA-binding agents [21,23].

In some cases, coordination to metal ions results in improvement of the pharmacological activity of organic compounds. In fact, as we previously reported, the antimicrobial activity of thiosemicarbazones significantly enhances upon coordination to copper(II) [24,25]. In a previous work we also demonstrated that upon complexation to *n*-butyltin and phenyltin the antibacterial and antifungal properties of 2-acetylpyridine-derived hydrazones substantially increase [26]. In addition, we also demonstrated that zinc(II) complexes with salicylaldehyde-derived hydrazones [27] proved to present a wider pharmacological profile as anti-inflammatory agents than their hydrazone ligands [28].

Here we report studies on the coordination of 2-acetylpyridine-phenylhydrazone (H2AcPh), 2-acetylpyridine-*para*-chloro-phenylhydrazone (H2Ac*p*ClPh), 2-acetylpyridine-*para*-nitro-phenylhydrazone (H2Ac*p*NO_2Ph), 2-benzoylpyridine-phenylhydrazone (H2BzPh), 2-benzoylpyridine-*para*-chloro-phenylhydrazone (H2Bz*p*ClPh) and 2-benzoylpyridine-*para*-nitro-phenylhydrazone (H2Bz*p*NO_2Ph) (see Fig. 1) to copper(II) as a strategy aimed to increase the hydrazones' antimicrobial activity. All compounds were tested against fungi *Candida albicans*, Gram-positive bacteria *Staphylococcus aureus* and *Enterococcus faecalis*, and Gram-negative bacteria *Pseudomonas aeruginosa*.

2. Materials and methods

2.1. Apparatus

All common chemicals were purchased from Aldrich and used without further purification. Partial elemental analyses were performed on a Perkin Elmer CHN 2400 analyzer. Thermo-gravimetric curves were obtained with a TGA50H thermo-balance (Shimadzu) in the 25–750 °C temperature range, under dynamic nitrogen atmosphere and at a heating rate of 10 °C min^{-1}. An YSI model 31

* Corresponding author. Tel.: +55 31 3409 5771; fax: +55 31 3409 5700.
E-mail address: hberaldo@ufmg.br (H. Beraldo).

0277-5387/$ - see front matter © 2012 Elsevier Ltd. All rights reserved.
http://dx.doi.org/10.1016/j.poly.2012.03.017

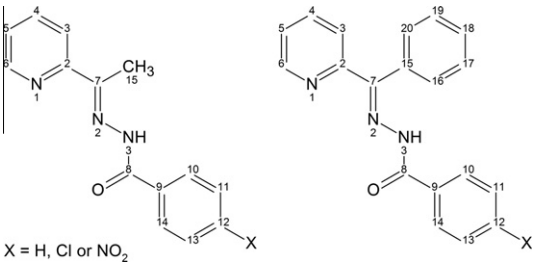

Fig. 1. Structural representation for 2-acetylpyridine- and 2-benzoylpyridine-derived hydrazones.

conductivity bridge was employed for molar conductivity measurements. Infrared spectra were recorded on a Perkin Elmer FT-IR Spectrum GX spectrometer using KBr plates (4000–400 cm^{-1}) and Nujol mulls between CsI plates (400–200 cm^{-1}). The molecular structure of a copper complex derived from complex (**3**), [Cu(2Ac*p*-NO_2Ph)Cl(DMSO)] (**3a**) (see Section 2.3), was investigated using single-crystal X-ray diffraction methods. The measurements were performed on an Enraf–Nonius Kappa-CCD diffractometer with graphite-monochromated Mo Kα (λ = 0.71073 Å) radiation. Diffraction data were obtained (φ and ω scans with κ-offsets) with COLLECT [29]. Integration and scaling of the reflections were performed with HKL DENZO-SCALEPACK suite of programs [30]. The unit cell parameters were obtained by least-squares refinement based on the angular settings for all collected reflections using HKL SCALEPACK [30]. The data were corrected numerically for absorption with PLATON [31]. The structure was solved by direct methods with SHELXS-97 [32] and the molecular model refined by full-matrix least-squares procedure on F^2 with SHELXL-97 [33].

Electron paramagnetic resonance (EPR) spectra were obtained on a Bruker ESP300E equipment with a frequency modulation of 100 kHz and a magnetic field modulation of 0.4–1 mT. Room temperature spectra of the samples in the solid state and as DMSO solutions (1 mmol L^{-1}) were obtained in glass capillaries of 1.2 mm internal diameter. Frozen DMSO solution spectra were acquired at liquid N_2 temperature (77 K) in 3 mm internal diameter Teflon® tubes.

2.2. Syntheses of 2-acetylpyridine-phenylhydrazone (H2AcPh), 2-acetylpyridine-para-chloro-phenylhydrazone (H2AcpClPh), 2-acetylpyridine-para-nitro-phenylhydrazone (H2AcpNO_2Ph), 2-benzoylpyridine-phenylhydrazone (H2BzPh), 2-benzoylpyridine-para-chloro-phenylhydrazone (H2BzpClPh) and 2-benzoylpyridine-para-nitro-phenylhydrazone (H2BzpNO_2Ph)

The syntheses of all hydrazones were performed as reported previously [26,34].

2.3. Syntheses of the copper(II) complexes with H2AcPh, H2AcpClPh, H2AcpNO_2Ph, H2BzPh, H2BzpClPh and H2BzpNO_2Ph

The copper(II) complexes were obtained by refluxing an ethanol solution of the desired ligand with copper chloride in 1:1 ligand-to-metal molar ratio. The solids were washed with ethanol followed by diethylether and then dried *in vacuo*.

*2.3.1. [Cu(2AcPh)Cl]·2H_2O (**1**) [chloro(2-acetylpyridinephenyl hydrazonato) copper(II)] dihydrate*

Green solid. Yield: 90%. *Anal.* Calc. ($C_{14}H_{16}ClCuN_3O_3$): C, 45.04; H, 4.32; N, 11.26. Found: C, 44.99; H, 4.29; N, 11.24%. Thermogravimetry (30–750 °C range): Calc. for weight loss of two water molecules: 9.64%. Found: 9.83%. Selected IR bands (cm^{-1}): ν(CN) 1600 m; ν(C=C) + ν(CN) 1586 m; 1566 m; ν(NC) 1493 s; ρ(py) 647 m; ν(Cu–N_{azom}) 415 m; ν(Cu–O) 332 s. Molar conductivity (1×10^{-3} mol L^{-1}, dimethylformamide, DMF): 37.50 Ω^{-1} cm^2 mol^{-1}.

*2.3.2. [Cu(2AcpClPh)Cl]·2H_2O (**2**) [chloro(2-acetylpyridine-para-chloro-phenylhydrazonato) copper(II)] dihydrate*

Green solid. Yield: 90%. *Anal.* Calc. ($C_{14}H_{15}Cl_2CuN_3O_3$): C, 41.24; H, 3.71; N, 10.31. Found: C, 41.50; H, 3.66; N, 10.26%. Thermogravimetry (30–750 °C range): Calc. for weight loss of two water molecules: 8.82%. Found: 8.94%. Selected IR bands (cm^{-1}): ν(CN) 1602 m; ν(C=C) + ν(CN); 1562 m; 1534 m; ν(NC) 1485 s; ρ(py) 644 m; ν(Cu–N_{azom}) 416 m; ν(Cu–O) 333 s. Molar conductivity (1×10^{-3} mol L^{-1}, dimethylformamide, DMF): 36.66 Ω^{-1} cm^2 mol^{-1}.

*2.3.3. [Cu(2AcpNO_2Ph)Cl] (**3**) [chloro(2-acetylpyridine-para-nitro-phenylhydrazonato) copper(II)]*

Green solid. Yield: 87%. *Anal.* Calc. ($C_{14}H_{11}ClCuN_4O_3$): C, 43.99; H, 2.90; N, 14.66. Found: C, 43.55; H, 2.84; N, 14.3%. Selected IR bands (cm^{-1}): ν(CN) 1600 m; ν(C=C) + ν(CN); 1568 m; 1527 m; ν(NC) 1495 m; ρ(py) 649 m; ν(Cu–N_{azom}) 417 m; ν(Cu–O) 326 s. Molar conductivity (1×10^{-3} mol L^{-1}, dimethylformamide, DMF): 5.28 Ω^{-1} cm^2 mol^{-1}.

Upon re-crystallization of complex (**3**) in 1:9 DMSO:acetone [Cu(2AcpNO_2Ph)Cl(DMSO)] (**3a**) was formed.

*2.3.4. [Cu(2BzPh)Cl] (**4**) [chloro(2-benzoylpyridinephenylhydrazonato) copper(II)]*

Green solid. Yield: 86%. *Anal.* Calc. ($C_{19}H_{14}ClCuN_3O$): C, 57.15; H, 3.53; N, 10.52. Found: C, 57.22; H, 3.41; N, 10.4%. Selected IR bands (cm^{-1}): ν(CN) 1596 m; ν(C=C) + ν(CN) 1596 m; 1552 m; 1487 m; ν(NC) 1494 s; ρ(py) 645 m; ν(Cu–N_{azom}) 421 m; ν(Cu–O) 304 s. Molar conductivity (1×10^{-3} mol L^{-1}, dimethylformamide, DMF): 21.56 Ω^{-1} cm^2 mol^{-1}.

*2.3.5. [Cu(2BzpClPh)Cl] (**5**) [chloro(2-benzoylpyridine-para-chloro-phenylhydrazonato) copper(II)]*

Green solid. Yield: 86%. *Anal.* Calc. ($C_{19}H_{13}Cl_2CuN_3O$): C, 52.61; H, 3.02; N, 9.69. Found: C, 52.75; H, 2.99; N, 9.85%. Selected IR bands (cm^{-1}): ν(CN) 1594 m; ν(C=C) + ν(CN) 1594 m; 1576 m; 1556 m; ν(NC) 1495 s; ρ(py) 645 m; ν(Cu–N_{azom}) 424 m; ν(Cu–O) 314 s. Molar conductivity (1×10^{-3} mol L^{-1}, dimethylformamide, DMF): 37.40 Ω^{-1} cm^2 mol^{-1}.

*2.3.6. [Cu(2BzpNO_2Ph)Cl] (**6**) [chloro(2-benzoylpyridine-para-nitro-phenylhydrazonato) copper(II)]*

Green solid. Yield: 74%. *Anal.* Calc. ($C_{19}H_{13}ClCuN_4O_3$): C, 51.36; H, 2.95; N, 12.61. Found: C, 51.21; H, 2.94; N, 12.15%. Selected IR bands (cm^{-1}): ν(CN) 1595 m; ν(C=C) + ν(CN) 1596 m; 1556 m; 1526 m; ν(NC) 1497 s; ρ(py) 647 m; ν(Cu–N_{azom}) 424 m; ν(Cu–O) 307 s. Molar conductivity (1×10^{-3} mol L^{-1}, dimethylformamide, DMF): 20.68 Ω^{-1} cm^2 mol^{-1}.

2.4. In vitro antimicrobial activity

Antimicrobial activity was evaluated by minimum inhibitory concentration (MIC) using the macro-dilution test [35]. *S. aureus* ATCC6538 and *P. aeruginosa* ATCC9027 were stored in Mueller Hinton Broth and *E. faecalis* ATCC19433 in Brain Heart Infusion. They were sub-cultured for testing in the same medium and grown at 37 °C. Then the bacterial cells were suspended, according to Clinical and Laboratory Standards Institute (CLSI) guidelines [36], to produce a suspension of about 10^5 CFU (colony forming units) mL^{-1}. *C. albicans* ATCC10231 stored in Sabouraud Broth was sub-cultured for testing in the same medium and grown at 37 °C. Then the yeast cells were suspended according to the McFarland protocol [36] in saline solution to produce a suspension of about 10^3 cells mL^{-1}.

For both the antibacterial and antifungal activity evaluations serial dilutions of the compounds, previously dissolved in DMSO, were prepared in test tubes. A 24-h old inoculum (100 μL) was added to each tube. The MIC, defined as the lowest concentration of the test compound which inhibits the visible growth after 20 h, was determined after incubation at 37 °C. Tests using tetracycline (in the case of *S. aureus*), ciprofloxacin (in the case of *E. faecalis*) or fluconazole (in the case of *C. albicans*) as reference and DMSO as negative control were carried out in parallel. The final DMSO concentration never exceeded 1%. In all cases no inhibition was observed with 5% v/v DMSO. All tests were performed in triplicates with full agreement among the results.

3. Results and discussion

Microanalyses suggest the formation of $[Cu(L)Cl]\cdot nH_2O$ ($n = 0$ or 2) complexes, in which the hydrazones coordinate as anionic ligands. The molar conductivity data reveal that the complexes are non-electrolytes, in accordance with the proposed formulations. Crystallization water molecules in complexes (**1**) and (**2**) were confirmed by thermo-gravimetric analyses.

3.1. Structural characterization of [Cu(2AcpNO$_2$Ph)Cl(DMSO)] (**3a**)

Crystal data and refinement results are summarized in Table 1. An ORTEP [37] drawing of **3a** is shown in Fig. 2 and bond distances and angles around the metal are in Table 2.

The copper(II) ion is in a fivefold distorted pyramidal environment, coordinated at the pyramid base to an anionic hydrazone molecule acting as a tridentate ligand through the pyridine and imine nitrogens [d(Cu–N1) = 2.049(2) Å, d(Cu–N2) = 1.936(2) Å] and the carbonyl oxygen [d(Cu–O1) = 1.994(1) Å], and to a chloride ion [d(Cu–Cl) = 2.2364(6) Å]. The pyramid apex is occupied by the oxygen atom of a DMSO molecule [d(Cu–O) = 2.267(2) Å]. On the pyramid base, *trans* O1–Cu–N1 and N2–Cu–Cl bond angles are 156.81(6) and 168.92(5)°, respectively, and *cis* L–Cu–L angles are in the 79.15(6)–100.21(4)° range. The tau parameter, $\tau = (\beta - \alpha)/60$ (β is the N2–Cu–Cl angle and α is the O1–Cu–N1 angle), which

Table 1
Crystal data and structure refinement results for [Cu(2AcpNO$_2$Ph)Cl(DMSO)] (**3a**).

Compound	[Cu(2AcpNO$_2$Ph)Cl(DMSO)] (**3a**)
Empirical formula	$C_{16}H_{17}ClCuN_4O_4S$
Formula weight	460.39
Temperature (K)	296(2)
Wavelength (Å)	0.71073
Crystal system	monoclinic
Space group	$P2_1/c$
Unit cell dimensions	
a (Å)	12.8481(4)
b (Å)	7.8598(2)
c (Å)	19.0296(5)
β (°)	107.587(2)
Volume (Å^3)	1831.85(9)
Z, D_{Calc} (mg/m^3)	4, 1.669
Absorption coefficient (mm^{-1})	1.483
F(000)	940
Crystal size (mm^3)	0.046 × 0.126 × 0.271
Crystal shape/color	prism/green
Theta range for data collection (°)	2.82–25.74
Index ranges	$-15 \leqslant h \leqslant 15$, $-9 \leqslant k \leqslant 9$, $-23 \leqslant l \leqslant 23$
Reflections collected/unique (R_{int})	18528/3478 (0.05)
Observed reflections [$I > 2\sigma(I)$]	2981
Completeness to $\theta = 26.00°$ (%)	99.0
Refinement method	Full-matrix least-squares on F^2
Weights, w	$[\sigma^2(F_o^2) + (0.0469P)^2 + 0.56P]^{-1}$ $P = [Max(F_o^2,0)+2F_c^2]/3$, $P = [Max(F_o^2,0)+2F_c^2]/3$
Data/restraints/parameters	3478/0/247
Goodness-of-fit on F^2	1.037
Final R indices[a] [$I > 2\sigma(I)$]	$R_1 = 0.0292$, $wR_2 = 0.0754$
R indices (all data)	$R_1 = 0.0364$, $wR_2 = 0.0800$
Largest difference in peak and hole (e Å^{-3})	0.232 and −0.677

[a] $R_1 = \Sigma||F_o| - |F_c||/\Sigma|F_o|$, $wR_2 = [\Sigma w(|F_o|^2 - |F_c|^2)^2/\Sigma w(|F_o|^2)^2]^{1/2}$.

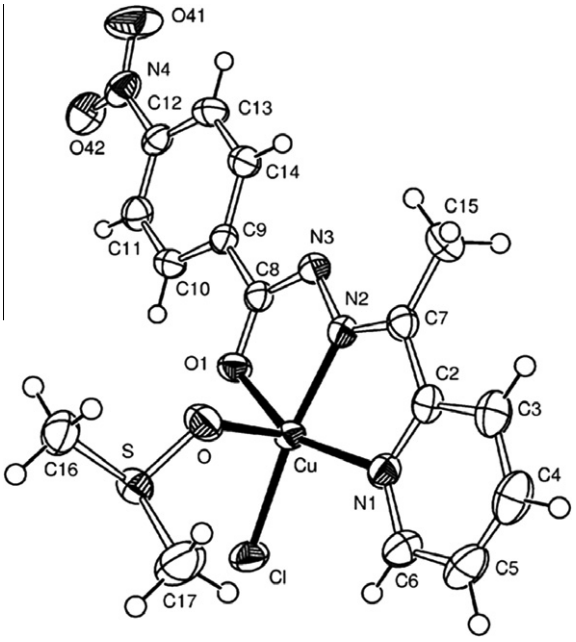

Fig. 2. Drawing of [Cu(2AcpNO$_2$Ph)Cl(DMSO)] (**3a**) showing the labeling of the non-H atoms and their displacement ellipsoids at the 50% probability level. Copper–ligand bonds are indicated by full lines.

Table 2
Selected bond distances (Å) and angles (°) in the molecular structures of [Cu(2FopNO$_2$Ph)Cl(DMSO)] and [Cu(2AcpNO$_2$Ph)Cl(DMSO)] (**3a**).

Compound	[Cu(2FopNO$_2$Ph)Cl(DMSO)] [39]	[Cu(2AcpNO$_2$Ph)Cl(DMSO)]
Bond lengths		
N1–C2	1.363(3)	1.356(3)
C2–C7	1.459(4)	1.474(3)
N2–C7	1.284(3)	1290(3)
N2–N3	1.363(3)	1.365(2)
N3–C8	1.331(3)	1.327(3)
O1–C8	1.285(3)	1.284(2)
Cu–N1	2.043(2)	2.049(2)
Cu–N2	1.942(2)	1.936(2)
Cu–O1	1.988(2)	1.994(1)
Cu–Cl	2.2354(7)	2.2364(6)
Cu–O	2.242(2)	2.267(2)
Bond angles		
N1–C2–C7	114.2(2)	115.00(17)
C2–C7–N2	114.8(2)	112.55(18)
C7–N2–N3	122.9(2)	122.01(17)
N2–N3–C8	107.3(2)	107.91(16)
N3–C8–O1	125.1(2)	125.45(18)
C6–N1–M	129.2(2)	127.86(16)
C2–N1–M	112.3(2)	112.19(13)
C7–N2–M	118.6(2)	120.32(14)
N3–N2–M	118.5(2)	117.66(12)
C8–O1–M	110.6(2)	109.70(13)
N1–Cu–N2	79.86(9)	79.24(7)
N2–Cu–O1	78.52(8)	79.15(6)
N1–Cu–O1	158.06(8)	156.81(6)
N2–Cu–Cl	162.64(7)	168.92(5)
O1–Cu–Cl	100.63(5)	100.21(4)
N1–Cu–Cl	98.88(6)	99.38(5)
N1–Cu–O	93.78(8)	88.56(6)
N2–Cu–O	95.06(8)	93.12(6)
O1–Cu–O	91.80(7)	100.91(6)
O–Cu–Cl	102.29(5)	97.84(4)

defines the degree of trigonality, was determined as 0.2018, in accordance with distorted square pyramidal structure [38].

The hydrazone anion is nearly planar [*rms* deviation of atoms from the least-squares plane of 0.060 Å] with the chlorine and metal ion laying close onto this plane [at 0.020(2) and 0.233(1) Å, respectively].

As expected, the molecular structure is very similar to the closely related [chloro(dimethylsulfoxide)(2-formylpyridine-*para*-nitrophenylhydrazonato) copper(II)] [Cu(2Fo*p*NO_2Ph)Cl(DMSO)], which only differs in that a H-atom rather than a methyl group is attached to the carbon C7 [39]. In fact, the best least-square superposition of the common skeletal structure of [Cu(2Ac*p*NO_2Ph)Cl] and [Cu(2Fo*p*NO_2Ph)Cl] [39] fragments, performed with the Kabsh's procedure [40], leads to a *rms* deviation between homologous non-H atoms of 0.142 Å. Small deviations are also observed when comparing the more weakly bonded DMSO apical ligand. In fact, the Cu–O bond distance is 0.025(2) Å larger in the present complex as compared with that containing the formyl derivative [39] and L–Cu–O bond angles differ in up to 9.11(8)°.

C8–O1 and C8–N3 distances of 1.284(2) and 1.327(3) Å are consistent with the formal partial double bond character expected upon deprotonation at N3 to form the anionic ligand.

3.2. Infrared spectra

The ν(C=C) + ν(C=N) composed mode observed at 1580–1585 cm^{-1} in the spectra of the hydrazones shifts to 1487–1604 cm^{-1} in the spectra of the complexes, indicating coordination of the azomethine nitrogen N2 [39,41]. The ν(C=O) absorption at 1660–1680 cm^{-1} in the spectra of the uncomplexed hydrazones disappears in those of the complexes, in agreement with coordination of an enolate oxygen. The pyridine in-plane deformation mode at 610–620 cm^{-1} in the spectra of the free hydrazones shifts to 644–649 cm^{-1} in those of the complexes, suggesting coordination of the heteroaromatic nitrogen [39,41]. New absorptions at 415–424 cm^{-1} and 286–305 cm^{-1} were attributed to ν(Cu-N) and ν(Cu–Npy) [42], respectively, and bands in the 305–333 cm^{-1} range were assigned to ν(Cu–O). Therefore, the infrared data for

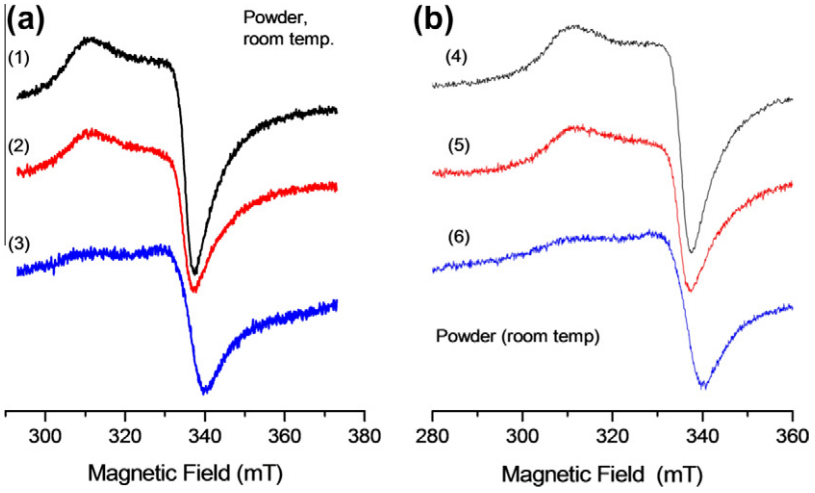

Fig. 3. EPR spectra of the Cu(II) complexes (**1**–**6**) in the solid state at room temperature.

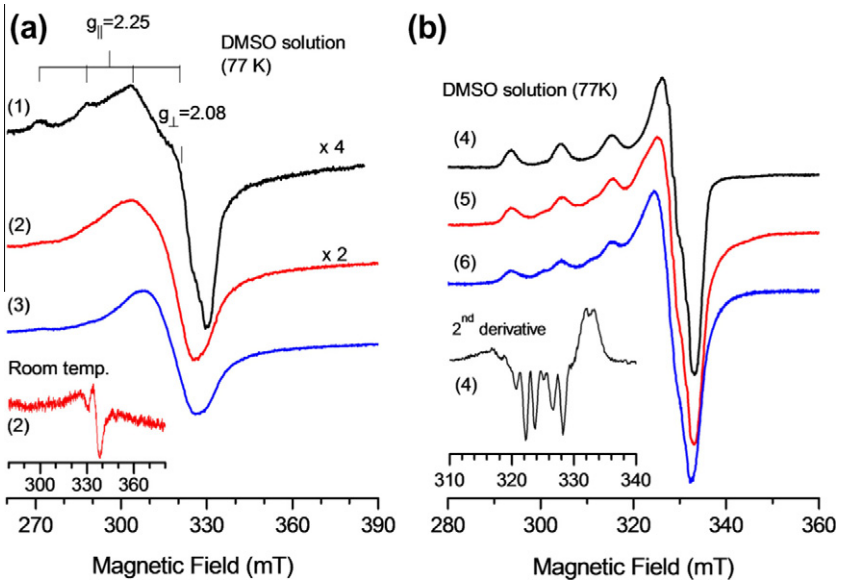

Fig. 4. EPR spectra of DMSO solutions of the Cu(II) complexes (**1**–**6**) (~1 mM) at 77 K. Insets: (a) room temperature spectrum of **2** in DMSO, (b) second derivative spectrum of **4** at the perpendicular region.

Table 3
Minimum inhibitory concentrations (MIC) of the hydrazones and their copper(II) complexes.

Compound	MIC ($\mu mol\ L^{-1}$)			
	S. aureus	*E. faecalis*	*P. aeuroginosa*	*C. albicans*
H2AcPh	428	>819	422	179
[Cu(2AcPh)Cl]·2H_2O (**1**)	49	131	>535	229
H2Ac*p*ClPh	197	>738	383	86
[Cu(2Ac*p*ClPh)Cl]·2H_2O (**2**)	10	122	>505	52
H2Ac*p*NO_2Ph	353	>696	337	111
[Cu(2Ac*p*NO_2Ph)Cl] (**3**)	>673	>523	>554	220
H2BzPh	177	>657	>670	105
[Cu(2BzPh)Cl] (**4**)	20	62	>510	107
H2Bz*p*ClPh	>619	>601	>613	69
[Cu(2Bz*p*ClPh)Cl] (**5**)	114.1	237	232	47
H2Bz*p*NO_2Ph	>600.5	>577	>577	>750
[Cu(2Bz*p*NO_2Ph)Cl] (**6**)	140.6	112	>441	306
$CuCl_2$·2H_2O	>656	>2322	>1255	>1671
Tetracycline hydrochloride	0.36	–	15	–
Fluconazole	–	–	–	79
Ciprofloxacin	–	0.25	–	–

the complexes indicate coordination of the hydrazones through the Npy–N–O chelating system and also the presence of a chloride ion at the fourth coordination site.

3.3. EPR spectra

The EPR spectra of **1**–**6** in the solid state at room temperature are presented in Fig. 3. They are all very similar, and are characteristic of mononuclear Cu(II) complexes with axial symmetry. The values of $g_{||}$ and $g_{\perp}$, 2.24 and 2.08, respectively, are in the range for this kind of complexes [43]. The values are consistent with a d_{x2-y2} ground state. The spectra lack the 4-line hyperfine splitting due to the interaction with Cu(II) nuclear magnetic moment ($I = 3/2$), as it is frequently the case for concentrated solid samples where exchange interactions are present [44,45]. Given that these are magnetically non-diluted systems, the lines are markedly broadened due to magnetic dipole–dipole interactions.

The EPR spectra of DMSO solutions of the complexes were recorded at 77 K (Fig. 4). The spectrum of **1** (Fig. 4a) is a superposition of an axially symmetric component that shows three of the 4-line hyperfine splitting, with parameters $g_{||} = 2.25$, $g_{\perp} = 2.08$, $A_{||} = 17.0$ mT, and a very broad component; those of **2** and **3** display only the broad component, where the parallel region is barely noticed. The spectra of **4**, **5** and **6** (Fig. 3b), however, do not present the broad component, and show the hyperfine splitting features at the parallel region. These results show that the complexes with 2-acetylpyridine derivatives aggregate in DMSO, while those with 2-benzoylpyridine derivatives do not, probably because of the bulkier substituents. Complex (**4**) presents a single component spectrum with $g_{||} = 2.265$, $g_{\perp} = 2.064$, and $A_{||} = 16.3$ mT. Complexes (**5**) and (**6**) display, besides the spectrum of complex (**4**), a second minor component with $g_{||} = 2.194$ and $A_{||} = 15.6$ mT, indicating two Cu(II) microenvironments.

Although Cu(II) interacts with at least two nonequivalent N atoms in complexes **1**–**6** (N_1 and N_2 in Fig. 2), the spectra of **1**–**3** do not exhibit resolved nitrogen super-hyperfine structure (Fig. 4a). Nitrogen super-hyperfine structure is noticed in the perpendicular region on the spectra of (**4**–**6**) (Fig. 4b). The inset presents the 2nd derivative spectrum of **4** at this region, which reveals the super-hyperfine splitting constant $A_N = 1.65$ mT, but the number of super-hyperfine lines is unclear mainly because of the unresolved hyperfine splitting at the perpendicular region.

DMSO solutions of the complexes at room temperature show identical broad EPR spectra (inset of Fig. 4a), indicating absence of motional narrowing.

3.4. Antimicrobial activity

The minimum inhibitory concentrations (MICs) of the hydrazones and their copper(II) complexes against *S. aureus*, *E. Faecalis*, *P. aureginosa* and *C. albicans* and are reported in Table 3.

The hydrazones showed poor activity against Gram-positive and Gram-negative bacteria with values of MIC higher than those of the control drugs. The compounds were inactive against *E. faecalis*. Nevertheless, they showed significant activity against *C. albicans*. In fact, the determined MIC values of H2Ac*p*ClPh (86 $\mu mol\ L^{-1}$) and H2Bz*p*ClPh (69 $\mu mol\ L^{-1}$), were comparable to that of the control drug fluconazole (MIC = 79 $\mu mol\ L^{-1}$). Hence the presence of a *para*-chloro substituent in the phenyl ring seems to contribute to an increase of antifungal activity in these compounds.

In general, the antimicrobial activities of the compounds improved after coordination to copper(II). The best results were obtained for complexes (**1**) (MIC = 49 $\mu mol\ L^{-1}$), (**2**) (MIC = 10 $\mu mol\ L^{-1}$) and (**4**) (MIC = 20 $\mu mol\ L^{-1}$) against *S. aureus*, and (**4**) (MIC = 62 $\mu mol\ L^{-1}$) against *E. faecalis*, respectively. Unfortunately, these MIC values are higher than those of the control drugs tetracycline (MIC = 0.36 $\mu mol\ L^{-1}$ against *S. aureus*) and ciprofloxacin (MIC = 0.25 $\mu mol\ L^{-1}$ against *E. faecalis*), respectively.

Complexes (**2**) (MIC = 52 $\mu mol\ L^{-1}$) and (**5**) (MIC = 47 $\mu mol\ L^{-1}$) were more active than their respective hydrazones (MIC = 86 and 69 $\mu mol\ L^{-1}$, respectively) against *C. albicans*. The MIC values of the hydrazones are similar to that of the control drug fluconazole (MIC = 79 $\mu mol\ L^{-1}$), while those of (**2**) and (**5**) are lower than that of fluconazole, hence suggesting that the complexes could be interesting as new antifungal drug candidates.

4. Conclusions

The studied 2-acetylpyridine- and 2-benzoylpyridine-derived hydrazones showed poor antimicrobial effect against Gram-positive *S. aureus* and *E. faecalis* and Gram-negative *P. aeruginosa* bacteria, but exhibited significant antifungal activity against *C. albicans*. In general, upon coordination to copper(II) the antibacterial effect against *S. aureus* and *E. faecalis* appreciably increased, although the MIC values for the complexes were higher than those determined for the control drugs tetracycline and ciprofloxacin. Coordination to copper(II) resulted in complexes with increased antifungal activity against *C. albicans* than fluconazole used as control.

As already mentioned, we demonstrated that upon coordination to copper(II) the antimicrobial activity of 2-acetylpyridine- and 2-benzoylpyridine-derived thiosemicarbazones increases [24,25]. The enhancement of the antimicrobial activities of hydrazone

analogs on complexation with copper(II) suggests that coordination of hydrazones to copper(II) could also represent an interesting strategy for antimicrobial dose reduction.

The increased use of antibacterial and antifungal agents in recent years has resulted in the development of resistance to these drugs. The important clinical implication of resistance has led to renewed interest in the development of novel antibacterial and antifungal agents [46]. Hence the studied compounds could constitute alternatives as drug candidates for the treatment of microbial diseases.

Acknowledgements

The authors are grateful to CNPq, INCT-INOFAR (Proc. CNPq 573.364/2008-6), FAPESP (Brazil) and to CONICET (Argentina) for financial support. O.E.P. is a Research Fellow of CONICET, Argentina. The authors thank Prof. Eliane Wajnberg for the use of the EPR spectrometer at CBPF, Centro Brasileiro de Pesquisas Físicas, and useful discussions.

Appendix A. Supplementary data

CCDC 863627 contains supplementary crystallographic data for [Cu(2Ac*p*NO_2Ph)Cl(DMSO)] (**3a**). These data can be obtained free of charge via http://www.ccdc.cam.ac.uk/conts/retrieving.html, or from the Cambridge Crystallographic Data Centre, 12 Union Road, Cambridge CB2 1EZ, UK; fax: +44 1223 336 033; or e-mail: deposit@ccdc.cam.ac.uk.

References

[1] A. Michalevičiūtė, R. Lygaitis, J.V. Gražulevičius, G. Buika, V. Jankauskas, A. Undzėnas, E. Fataraitė, Synthetic Met. 159 (2009) 223.
[2] G.A. Ibañez, G.M. Escandar, A.C. Olivieri, J. Mol. Struct. 605 (2002) 17.
[3] S. Rollas, N. Gulerman, H. Erdeniz, Farmaco 57 (2002) 171.
[4] P. Vicini, F. Zani, P. Cozzini, I. Doytchinova, Eur. J. Med. Chem. 37 (2002) 553.
[5] E. Viñuelas-Zahínos, M.A. Maldonado-Rogado, F. Luna-Giles, F.J. Barros-Garcia, Polyhedron 27 (2008) 879.
[6] N. Karali, A. Kocabalkanli, A. Gürsoy, Ö. Ates, Farmaco 57 (2002) 589.
[7] D. Sriram, P. Yogeeswari, R.V. Devakaram, Bioorg. Med. Chem. 14 (2006) 3113.
[8] D. Sriram, P. Yogeeswari, K. Madhu, Bioorg. Med. Chem. Lett. 16 (2006) 876.
[9] S.K. Sridhar, S.N. Pandeya, J.P. Stables, A. Ramesh, Eur. J. Pharm. Sci. 16 (2002) 129.
[10] S.G. Küçükgüzel, A. Mazi, F. Sahin, S. Öztürk, J. Stables, Eur. J. Med. Chem. 38 (2003) 1005.
[11] A.R. Todeschini, A.L.P. de Miranda, K.C.M. da Silva, S.C. Parrini, E.J. Barreiro, Eur. J. Med. Chem. 33 (1998) 189.
[12] H.J.C. Bezerra-Netto, D.I. Lacerda, A.L.P. Miranda, H.M. Alves, E.J. Barreiro, C.A.M. Fraga, Bioorg. Med. Chem. 14 (2006) 7924. and references therein.
[13] O.I. El-Sabbagh, H.M. Rady, Eur. J. Med. Chem. 44 (2009) 3680.
[14] P. Vicini, M. Incerti, P. La Colla, R. Loddo, Eur. J. Med. Chem. 44 (2009) 1801.
[15] P. Vicini, M. Incerti, I.A. Doytchinova, P. La Colla, B. Busonera, R. Loddo, Eur. J. Med. Chem. 41 (2006) 624.
[16] M. Varache-Lembège, S. Moreau, S. Larrouture, D. Montaudon, J. Robert, A. Nuhrich, Eur. J. Med. Chem. 43 (2008) 1336.
[17] P.V. Bernhardt, L.M. Caldwell, T.B. Chaston, P. Chin, D.R. Richardson, J. Biol. Inorg. Chem. 8 (2003) 866.
[18] N. Filipović, H. Borrmann, T. Todorović, M. Borna, V. Spasojević, D. Sladić, I. Novaković, K. Andjelković, Inorg. Chim. Acta 362 (2009) 1996.
[19] M.C. Rodríguez-Argüelles, S. Mosquera-Vásquez, P. Tourón-Touceda, J. Sanmartin-Matalobos, A.M. García-Deibe, M. Belicchi-Ferrari, J. Inorg. Biochem. 101 (2007) 138.
[20] M.A. Affan, S.W. Foo, I. Jusoh, S. Hanapi, E.R.T. Tiekink, Inorg. Chim. Acta 362 (2009) 5031.
[21] Z.Y. Yang, B.D. Wang, Y.H. Li, J. J. Organomet. Chem. 691 (2006) 4159.
[22] D.K. Johnson, T.B. Murphy, N.J. Rose, W.H. Goodwin, L. Pickart, Inorg. Chim. Acta 67 (1982) 159.
[23] V. Mahalingam, N. Chitrapriya, F.R. Fronczek, K. Natarajan, Polyhedron 27 (2008) 1917.
[24] I.C. Mendes, J.P. Moreira, A.S. Mangrich, S.P. Balena, B.L. Rodrigues, H. Beraldo, Polyhedron 26 (2007) 3263.
[25] I.C. Mendes, J.P. Moreira, N.L. Speziali, A.S. Mangrich, J.A. Takahashi, H. Beraldo, J. Braz. Chem. Soc. 17 (2006) 1571.
[26] A.A. Recio-Despaigne, L.F. Vieira, I.C. Mendes, F.B. Da Costa, N.L. Speziali, H. Beraldo, J. Braz. Chem. Soc. 21 (2010) 1247.
[27] G.L. Parrilha, R.P. Vieira, A.P. Rebolledo, I.C. Mendes, L.M. Lima, E.J. Barreiro, O.E. Piro, E.E. Castellano, H. Beraldo, Polyhedron 30 (2011) 1891.
[28] W. Bispo Júnior, M.S. Alexandre-Moreira, M.A. Alves, A. Perez-Rebolledo, G.L. Parrilha, E.E. Castellano, O.E. Piro, E.J. Barreiro, L. Moreira Lima, H. Beraldo, Molecules 16 (2011) 6902.
[29] Enraf-Nonius (1997–2000), COLLET, Nonius BV, Delft, The Netherlands.
[30] Z. Otwinowski, W. Minor, in: C.W. Carter Jr., R.M. Sweet (Eds.), Methods in Enzymology, vol. 2, Academic Press, New York, 1997, p. 307.
[31] A.L. Spek, PLATON, A Multipurpose Crystallographic Tool, Utrecht University Utrecht, The Netherlands, 1998.
[32] G.M. Sheldrick, SHELXS-97, Program for Crystal Structure Resolution, University of Göttingen, Göttingen, Germany, 1997. See also: G.M. Sheldrick, Acta Crystallogr., Sect. A46 (1990) 467–473..
[33] G.M. Sheldrick, SHELXS-97, Program for Crystal Structure Resolution, University of Göttingen, Göttingen, Germany, 1997. See also: G.M. Sheldrick, Acta Crystallogr., Sect. A64 (2008) 112–122.
[34] A.A. Recio-Despaigne, J.G. Da Silva, A.C.M. Do Carmo, O.E. Piro, E.E. Castellano, H. Beraldo, Inorg. Chim. Acta 362 (2009) 2117.
[35] National Committee for Clinical Laboratory Standards, Method for dilution antimicrobial susceptibility tests for bacteria that grow aerobically, in: NCCLS Document M7–A6, Pennsylvania, USA, 2003, ISBN: 1-56238-486-4.
[36] National Committee for Clinical Laboratory Standards, Reference method for broth dilution antifungal susceptibility testing of yeasts, in: NCCLS Document M27eMA2 NCCLS, Pennsylvania, USA, 2002, ISBN: 1-56238-469-4.
[37] C.K. Johnson, ORTEP. Report ORNL-5138, Oak Ridge, TN, 1976.
[38] A.W. Addison, R.T. Nagaswara, J. Reedijk, J. Van Rijn, G.C. Verschoor, J. Chem. Soc., Dalton Trans. 7 (1984) 1349.
[39] A.A. Recio-Despaigne, J.G. Da Silva, A.C.M. Do Carmo, F. Sives, O.E. Piro, E.E. Castellano, H. Beraldo, Polyhedron 28 (2009) 3797.
[40] W. Kabsch, Acta Crystallogr., Sect. A32 (1976) 922.
[41] A.A. Recio-Despaigne, J.G. Da Silva, A.C.M. Do Carmo, O.E. Piro, E.E. Castellano, H. Beraldo, J. Mol. Struct. 920 (2009) 97.
[42] K. Nakamoto, Infrared and Raman Spectra of Inorganic and Coordination Compounds, forth ed., Wiley, New York, 1986.
[43] P.R. Bontchev, B.B. Ivanova, R.P. Bontchev, D.R. Mehandjiev, Polyhedron 20 (2001) 231.
[44] B.J. Hathaway, D.E. Billing, Coord. Chem. Rev. 5 (1970) 143.
[45] K.O. Ferraz, S.M.S.V. Wardell, J.L. Wardell, S.R.W. Louro, H. Beraldo, Spectrochimica Acta Part A 73 (2009) 140.
[46] M.A. Ghannom, L.B. Rice, Clin. Microbiol. Rev. 12 (1999) 501.